Supersonic Vehicle Configuration Transitions to Enable Supersonic Retropropulsion during Mars Entry, Descent, and Landing

David Blette
Georgia Institute of Technology
North Ave NW
Atlanta, GA 30332
404-894-2000
dblette@gatech.edu

Robert Braun
Georgia Institute of Technology
North Ave NW
Atlanta, GA 30332
404-894-2000
robert.braun@aerospace.gatech.edu

***Abstract*— This paper investigates types of supersonic vehicle configuration transition events necessary to initiation supersonic retropropulsion as part of human-class Mars entry, descent, and landing. This research assumes an entry vehicle with a 105 mT entry mass and an ellipsled aeroshell similar to the NASA EDL Design Reference Architecture 5.0. All entry architectures are assumed all-propulsive. Three transition architectures are considered: a pitch-around maneuver, an aeroshell front-exit, and an aeroshell hinged-exit. Propulsive subsystem thrust requirements are defined for the pitch-around maneuver. For transitions involving solid mass ejections, debris flight envelopes are determined and compared to a descent vehicle trajectory under a modified gravity turn. It is shown that far-field recontact risks exist for the proposed architectures involving solid mass ejections and recontact mitigation schemes are required.**

TABLE OF CONTENTS

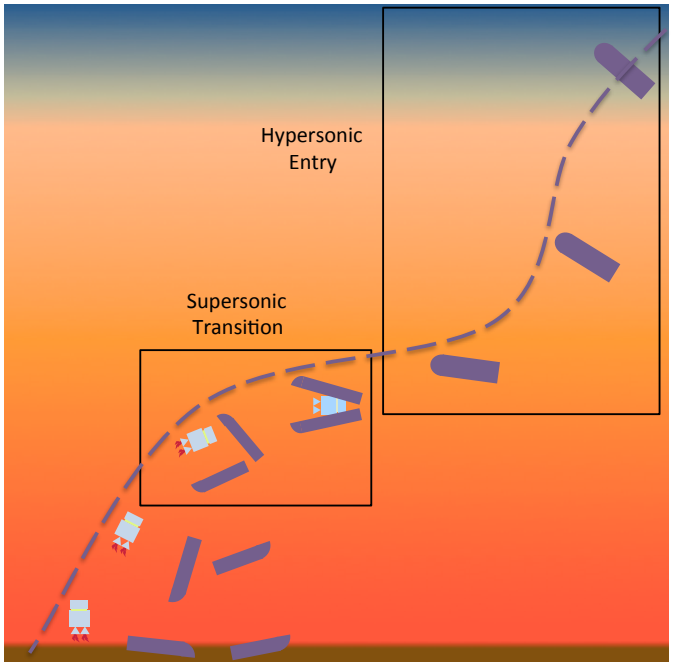

Figure 1. A hypothetical Mars entry trajectory profile exemplifying the stages of entry vehicle configurations

1. INTRODUCTION

The landing of the Mars Science Laboratory (MSL) represents the current state-of-the-art in EDL technologies for Mars exploration. MSL decelerated a 0.9 mT payload to -4.5 km altitude [1] to within 10 km of a desired target [2] using a 4.5 m diameter rigid aeroshell and a 21.5 m disk-gap-band supersonic parachute [3]. Every mission that has successfully landed a payload on Mars has utilized similar heritage deceleration technologies from the 1960's and 1970's Viking era. Utilizing only Viking heritage deceleration technologies presently available, it is estimated that a 1.1 mT payload landed at 0 km elevation represents the upper limit of current EDL capabilities [4]. The succession from the current state-of-the-art along NASA's goal of extending and sustaining human presence in our solar system will require landing large robotic (10 mT) and human class payloads (40-80 mT) on Mars with landed accuracies on the order of meters.

Supersonic retropropulsion (SRP) is a promising technology currently under heavy development by NASA that is envisioned to bridge the gap between the current state-of-the-art and future required EDL performance to enable high-mass Mars missions. SRP extends propulsive deceleration beyond subsonic flight conditions into the supersonic flight regime. Previous landed Mars missions have used propulsive deceleration in the subsonic flight regime by subsonically transitioning from a hypersonic entry vehicle configuration into a descent vehicle configuration in which propulsive deceleration systems thrust into the oncoming atmospheric flow. Initiating propulsive deceleration earlier in flight provides more total deceleration and increases landed mass capabilities [5]. However, initiating propulsive deceleration during supersonic flight also requires supersonically transitioning a hypersonic entry vehicle configuration into a propulsive deceleration configuration. Figure 1 depicts a typical Mars entry trajectory profile and identifies the point in the trajectory where a vehicle transitions between the hypersonic entry configuration and the powered descent configuration that touches down on the planet's surface.

Supersonic transitions have never been accomplished at Mars and involve different dynamics and challenges as compared

978-1-4673-7676-1/16/$31.00

to subsonic transitions due to the fundamental difference between supersonic and subsonic atmospheric flight. Jettisoning solid mass at supersonic speeds represents a primary challenge to accomplishing supersonic vehicle configuration transitions. All atmospheric vehicle configuration transitions on Mars have occurred in subsonic flight regimes. These transition schemes used combinations of Viking heritage technologies such as pyrotechnic separations, spring systems, and guide rails to separate the forebody heatshield from the vehicle descent stage [6]. According to Ref. [6], the dynamic complexity of atmospheric EDL separation events is increased due to atmospheric forces exerted on an EDL system during heatshield jettison as well as the need to mitigate potential recontact risks for both the near and far-field trajectories of the descent vehicle and jettisoned solid mass. Due to fundamental differences between supersonic and subsonic fluid flows, separation complexity and risk are increased during supersonic transitions. Analysis must be performed to determine the feasibility of supersonic transitions in order to enable SRP as a flight ready deceleration technology.

Previous studies focusing on high-mass Mars EDL utilizing SRP have either assumed an instantaneous supersonic transition between vehicle configurations or have made a free-fall assumption to conservatively approximate the flight performance of a transition [4]. A free-fall assumption assumes that the transition between the hypersonic entry configuration and the SRP initiation configuration is conservatively modeled by allowing the entry vehicle to fall only under the influence of gravity while both aerodynamic forces and thrust forces are turned off. Free-fall results in a decrease in altitude and an increase in velocity that is believed to be a conservative estimate of the post-transition state of a descent vehicle. Analyses utilizing these free-fall assumptions have made no attempt to model or characterize the multi-body dynamics of the descent vehicle or jettisoned debris during vehicle configuration transitions. These analyses have simply assumed the entry vehicle begins the transition in the hypersonic configuration and ends the transition in the powered descent configuration with no regard to how this change was physically accomplished. To accurately model the performance and feasibility of a supersonic transition, analysis is required to characterize solid mass jettison recontact risks and to determined subsystem performance requirements to successfully complete a supersonic solid mass jettison and mitigate recontact risks.

Jettisoned mass recontact risks may be categorized into near-field and far-field risks. Near-field risks are those that concern the initial jettison of solid mass from a descent vehicle. Jettisoning an aeroshell away from a descent vehicle requires subsystems capable of pushing a large piece of mass that was once protecting the descent vehicle during hypersonic entry far enough away from the descent vehicle so that powerful retro-rockets can be ignited to slow the vehicle down. Moving a large piece of mass away from a descent vehicle at supersonic speeds involves complex dynamics. If the ejected mass is not carefully controlled, it could strike the descent vehicle, causing massive damage or catastrophic mission failure. Far-field risk are concerned with recontact risk after a piece of solid mass has been successfully ejected, the descent vehicle has initially cleared the ejected mass, and retropropulsion has been initiated. Depending on the flight dynamics of the descent vehicle and each piece of ejected solid mass, the ejected debris might recontact the descent vehicle on its trajectory toward the planet surface. Additionally, the ejected debris could also pose a threat to any pre-deployed assets on the ground (e.g. human habitats and power generators) near the descent vehicle's target landing site.

Table 1. DRA 5.0 Vehicle Specifications

Parameter	Value
Initial Mass	105 mT
Total Descent Thrust	1200 kN
Isp	360 s

Table 2. Supersonic Transition Initial Trajectory Conditions

Parameter	Value
Velocity	680 m/s
Mach	3.35
FPA	-9.97°
Altitude	8.7 km
Dyn. Pressure	2 kPa

This paper investigates far-field recontact risks for several proposed supersonic vehicle configuration transition schemes. Analysis considers the range of aerodynamic coefficients possible for different types of ejected debris and then compares possible debris extremum trajectories to the descent vehicle trajectory in order to determine whether far-field recontact risks exist. Additionally, this paper looks at subsystem performance requirements for one proposed transition scheme that does not require any solid mass ejections. Analysis investigates aerodynamic forces imparted on the descent vehicle during the transition to determine the reaction control subsystem propulsive thrust performance necessary to enable the transition. Future work will investigate near-field recontact risks and mitigation techniques for far-field recontact risks.

Section 2 of this paper identifies the reference entry vehicle used throughout this study and discusses the assumptions made during the performed analyses. It identifies the three proposed supersonic vehicle configuration transition schemes that are analyzed in this paper. It discusses the development of aerodynamic databases for pieces of ejected solid mass debris and describes the trajectory simulation used throughout this investigation. Section 3 discusses the simulation results obtained during this investigation. Section 4 summarizes the conclusions of this research and discusses future work.

2. ASSUMPTIONS AND SIMULATION MODELING

Assumptions

The reference entry vehicle for this investigation is a 10x30m Ellipsled based on the NASA Design Reference Architecture 5.0 (DRA 5.0) vehicle. The vehicle specifications are provide in table 1. Trajectory parameters at the start of each supersonic transition are taken from the DRA 5.0. The initial DRA 5.0 study assumed a 20 second free-fall preceding SRP initiation in place of performing a supersonic vehicle configuration transition analysis. Trajectory parameters at the start of each supersonic transition for the current analyses are assumed to be those of the DRA 5.0 trajectory immediately before the 20 second free-fall. These conditions are summarized in table 2.

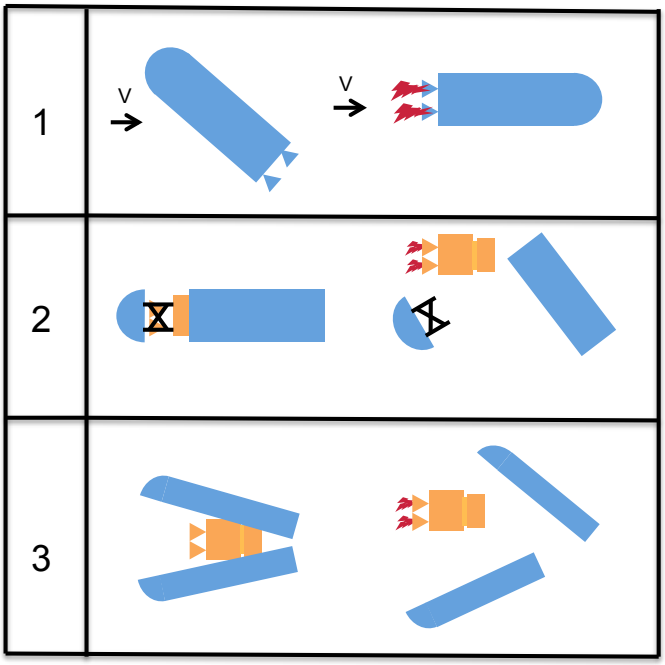

Figure 2. Concept of operations of the three transition architectures investigated in this study

Proposed Vehicle Transition Schemes

Figure 2 depicts the three transition architectures considered in this work. The first transition depicted in Figure 2 is termed a "pitch-around maneuver". In this transition scheme the hypersonic entry vehicle begins the transition at the trimmed hypersonic angle of attack of 45°. Using reaction control system (RCS) thrusters, the entry vehicle pitches around until achieving a 180° angle of attack with the descent engines directed into the oncoming flow. At this point the transition phase terminates and powered descent phase initiates. The second transition depicted in Figure 2 is termed a "front exit". In this transition scheme, the front hemispherical cap separates from the rear cylindrical portion of the aeroshell but remains attached to the descent vehicle contained within the aeroshell. Together, the descent vehicle and the hemispherical cap slide out of and away from the cylindrical aft-shell. Once clear of the aft-shell, the hemispherical cap separates from the descent vehicle. After the descent vehicle is clear of both the hemispherical cap and the aft-shell, the transition phase is over and the powered descent phase begins. The third transition depicted in Figure 2 is termed a "hinged exit". In this transition scheme, the hypersonic aeroshell is split along its symmetry axis and then opens up like a clamshell. The descent vehicle then emerges from the clamshell and once clear, begins the powered descent phase.

The pitch-around maneuver benefits from not having any ejected debris and therefore near-field and far-field debris recontact risks to not exist. Possible downsides of this maneuver include the need for powerful RCS thrusters which absorb available payload mass. The front-exit and hinged-exit maneuvers both eject debris during transitions and therefore suffer from potential near-field and far-field recontact risks. Analysis is required to characterize the recontact risk posed by the ejected debris and subsequent recontact mitigation techniques must be developed if recontact risks exist.

Aerodynamic Database and Numeric Trajectory Simulation

An aerodynamic database was compiled using the industry standard NASA tool Configuration Based Aerodynamics (CBAERO). CBAERO utilizes panel methods to determine inviscid newtonian aerodynamics. The resulting aerodynamics are considered accurate for supersonic speeds. This study utilizes CBAERO aerodynamics throughout the entire flight regime. While the accuracy of these aerodynamics drops off in the lower transonic flight regime, they may still be used to obtain useful results. All simulated debris trajectories are terminated when speeds drop below mach 1, as the results cannot be considered reliable in the subsonic flight regime.

A three-degree-of-freedom numeric trajectory simulation was developed to analyze the motion of ejected debris and the descent vehicle under a modified gravity turn control law. The modified gravity turn control law assumes constant thrust during deceleration and optimizes the angle the thrust vector makes with the horizon in order to zero out the horizontal and vertical velocity while minimizing propellant mass used. This control law was developed at the Jet Propulsion Laboratory for related supersonic retropropulsion mission design work. The simulation is coded in Matlab and the equations of motion are integrated using a fourth-order Runge-Kutta variable time step scheme. An exponential Martian atmosphere is assumed with a scale height of 10.8 km. An inverse-square law gravity model is assumed with a surface gravity of 3.711 m/s^2 and a mean planetary radius of 3390 km.

3. Simulation Results

Pitch-Around Maneuver

Figure 3(a) shows aerodynamic moments (solid) and required applied moments (dashed) to complete pitch-around maneuvers for three different constant angular accelerations. These results do not represent what actual moments would be required to pitch around the DRA 5.0 reference vehicle, but provide an approximation of the range of moments that could be expected during such a maneuver. In this figure, the reference vehicle is pitched around from an initial hypersonic trimmed angle of attack (AoA) of 45° with a constant angular acceleration until the vehicle reaches 180° AoA. Note that under these modeling assumptions, the reference vehicle will reach 180° AoA with a non-zero angular velocity, as no control scheme is implemented to ensure the vehicle reaches 180° AoA with zero angular velocity. The vehicle reaches 180° AoA with an angular velocity equal to the time duration of the maneuver multiplied by the constant angular acceleration. Note, ensuring a zero angular velocity at 180° AoA would require decelerating the vehicle's angular velocity which would result in longer transition times and higher propellant mass for the same maneuver.

Performing a pitch-around maneuver at higher angular accelerations results in shorter maneuver times and higher peak applied moments. Figure 3(b) shows the thrust that would be required to perform each pitch-around maneuver based on the trends in figure 3(a) and a 10m moment arm from the vehicle center of gravity about which RCS thrusters apply force. The reference vehicle is 30m long and the center of gravity is located approximately 16m from the base of the vehicle. Therefore, a RCS placement 10m ahead of the center of gravity is judged to be ambitious. Figure 3(b) shows that 160 kN of peak force is required from the RCS thrusters to achieve a pitch-around maneuver at 1 deg/s^2 and 430 kN of peak force is required for a maneuver at 5

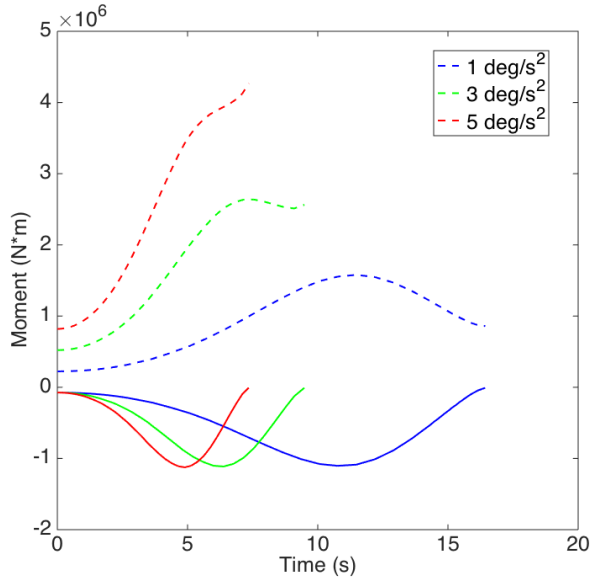

(a)Aerodynamic moments (solid) and commanded moments (dashed)

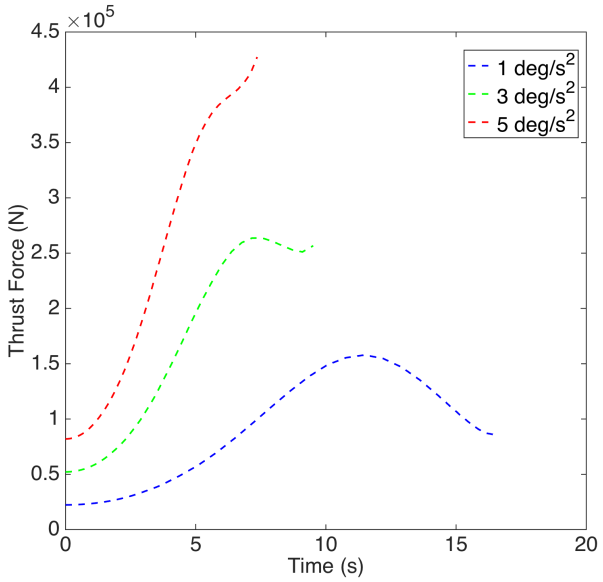

(b)Commanded thrust force base on 10m moment arm

Figure 3. Moments and thrust forces for the pitch-around maneuver

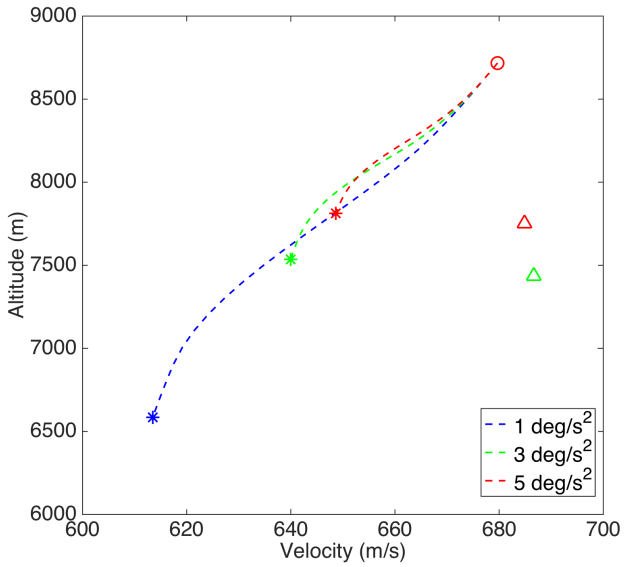

(a)Pitch-around maneuver

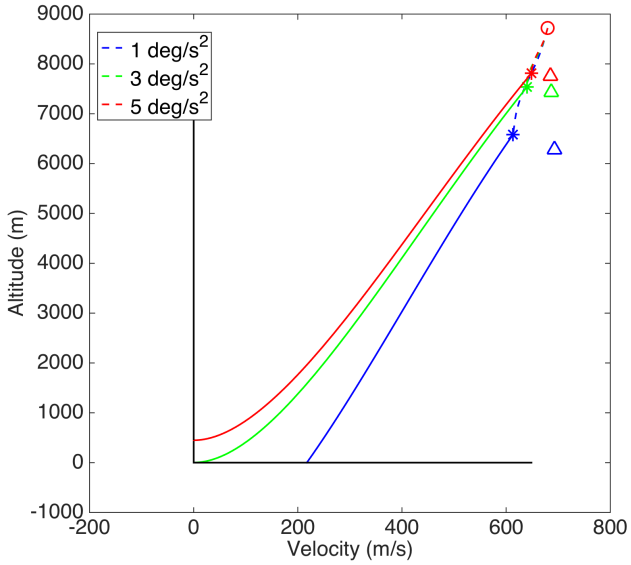

(b)Gravity turn to zero altitude

Figure 4. Altitude-velocity space for the pitch-around maneuver and subsequent gravity turn to zero altitude

deg/s^2. Reference [4] identifies the state-of-the-art for high thrust RCS engines as a 90kN Korean engine. Additionally, specifications for the initial DRA 5.0 design only required 9kN RCS thrusters for roll/pitch control and a 62kN RCS thruster for yaw control. Depending on vehicle structural, packaging, and mass constraints, one can imagine utilizing several RCS engine thrusters to perform a maneuver. Based on the current analysis, a maneuver at 5 deg/s^2 would require five state-of-the-art RCS thrusters thrusting in the same direction. Additionally, in order to arrive at 180° AoA with zero angular velocity, additional RCS engines would be required to decelerate the vehicle. The results of this analysis show that RCS thrust requirements far exceed the requirements envisioned in the initial DRA 5.0 study.

Figure 4(a) shows altitude velocity space for pitch-around maneuvers at different angular accelerations. The circular data point indicates the common starting point of the pitch-around maneuvers and the colored asterisks indicate respective maneuver ending points. Previous analyses that consider SRP trajectory performance have commonly modeled the transition between the hypersonic entry vehicle configuration and SRP initiation vehicle configuration via a free-fall for a specified amount of time, typically 20 seconds. To draw comparisons between transition performance of previous analyses in the literature and a pitch-around maneuver, colored triangle data points indicate respective terminal conditions if the vehicle had been in free-fall for a duration equal to the respective pitch-around maneuver duration. In all cases,

an increase in maneuver duration results in a lower terminal altitude and velocity for the simulated pitch-around. Free-fall assumptions always results in conservative terminal conditions with respect to simulated pitch-around maneuvers - the pitch-around maneuver always has lower terminal velocity and higher terminal altitude.

Figure 4(b) extends the results in figure 4(a) by adding a propulsive descent phase starting from the pitch-around transitional maneuver terminal conditions. The propulsive descent control logic assumes constant thrust at an optimized thrust angle that minimizes propellant mass while nulling out horizontal and vertical velocity. The propulsive descent thrust force is given in table 1. Figure 4(b) shows that increasing transition maneuver duration results in lower landed altitudes. This analysis assumed a spherical planet and an exponential atmosphere. Based on these results, the 5 deg/s^2 pitch-around maneuver is the only maneuver capable of landing above 0 km altitude with 0 m/s velocity.

This analysis shows that pitch-around maneuvers suffer from competing performance metrics. Increasing landed mass or landed altitude requires increasing the transition angular acceleration. Higher transitional angular accelerations quickly increase required thrust level from an RCS system. The thrust levels necessary to complete a transition quickly become prohibitively large - requiring on the order of 400 kN for a 5 deg/s^2 transition. Optimizing the thrust profile and using non-constant angular accelerations may reduce thrust requirements. However, optimized results will still be of the same order of magnitude as the results presented here due to strong aerodynamic forces and moments acting on the vehicle and the necessity to complete the transition within reasonable time constraints. The results presented here show that required subsystem thrust performance necessary to utilize a pitch-around maneuver for this reference vehicle is beyond the current state-of-the-art.

Hinged Exit Maneuver

The pitch-around maneuver does not involve any solid mass ejection as part of its transition scheme and therefore an investigation of the recontact risks of the ejected debris is not required. The hinged exit transition scheme simultaneously ejects the aeroshell as two similar pieces of solid debris and therefore a debris recontact risk investigation is required. This section presents an investigation into debris far-field recontact risks by looking at possible trajectory dispersions of the ejected debris as compared to the trajectory of the descent vehicle. This analysis assumes that both pieces of debris have successfully ejected from the descent vehicle and have overcome any possible near-field recontact risks, which are not investigated in this paper. The hinged exit transition scheme ejects two identical pieces of debris - as such, trajectories for just one of these pieces are simulated in this analysis. It is assumed that the trajectories for the simulated single piece of debris describe the trajectory dispersions and recontact risks of both pieces of debris after simultaneous ejection during the hinged exit transition scheme.

In figures 5(a), 6(a), and 7(a), the descent vehicle trajectory is represented by a single trajectory following the previously described gravity turn control logic. Six trajectories are presented for each single piece of ejected debris. To determine the landing footprint of the each ejected debris, trajectories are simulated for combinations of maximum drag, minimum drag, maximum lift, minimum lift, and zero lift. The maximum and minimum values for lift and drag were

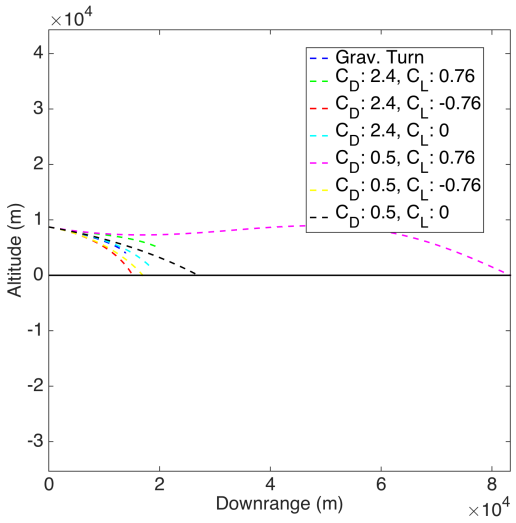

(a)

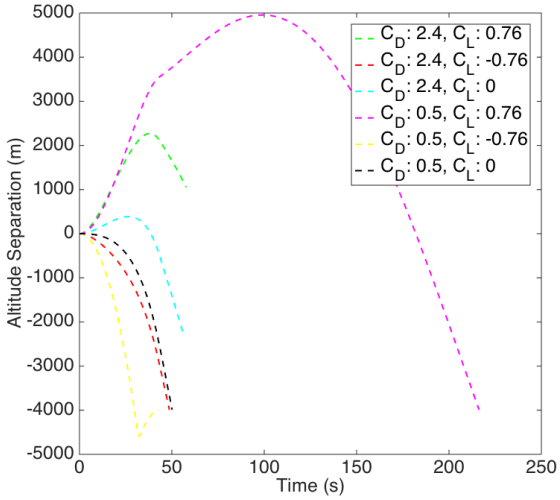

(b)

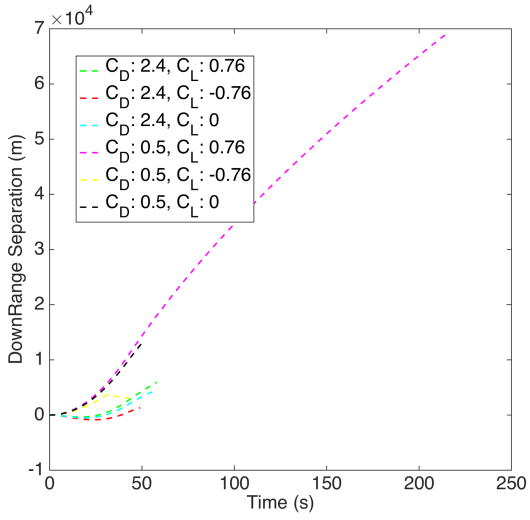

(c)

Figure 5. Trajectory dispersions for the hinged exit transition scheme

determined from the range of possible debris flight conditions for angles of attack between 0 and 360 degrees, mach numbers between 2 and 5, and dynamic pressures between 100 and 10000 Pascal. Each aerodynamic coefficient extremum does not necessarily correspond to the same flight conditions or angle of attack as another extremum; each value independently represents the extremum of possible values for that specific coefficient. For example, the combination of maximum drag and maximum lift may not be physically achievable at any single fight condition, but each value will occur independently in the range of flight conditions. This method of characterizing extremum values is selected over the alternative method of determining the extremum values based on the range of trimable aerodynamic states for several reasons. This study is aimed at determining the extremum of the possible flight envelope of a piece of debris in order to determine whether or not far-field recontact risks exit. This study does not currently model debris to have any flight control subsystems (e.g. aerodynamic control surfaces or propulsion systems). Furthermore, based on future near-field recontact risk analysis, the initial orientation and angular rates of ejected debris may or may not be known or controllable at the time of debris ejection. Under these conditions, it is not evident whether or not the debris will stabilize in a trimmed state or in a range of trimable states during flight. Therefore, this analysis assumes that the debris are in a tumbling trajectory and likely to experience a wide array of drag forces and lift-to-drag ratios during flight. It is not practical to apply any type of probability distribution to characterize the range aerodynamic states experienced during tumbling flight, therefore the method of determining the debris extremum flight envelope is chosen as described above in order to ensure that identified flight envelopes encompasses all possible practical flight envelopes. In other words, the method was chosen to be very conservative. Future investigations of mitigation techniques will consider controlling debris flight envelopes using flight control subsystems in order to avoid recontact risks with the descent vehicle.

Figure 5(a) shows the altitude and downrange space of the descent vehicle and the ejected debris. As mentioned previously, debris trajectories are terminated when they move below mach 1 as the aerodynamic database is not reliable for subsonic speeds. As seen in the figure, the simulated debris trajectories envelop the descent vehicle gravity turn trajectory. From this figure, it is evident that in the absence of descent vehicle divert maneuvers or debris flight control schemes, the debris landing footprint poses a direct threat to the descent vehicle landing site and any pre-deployed landed assets near the descent vehicle landing site.

Figure 5(b) and 5(c) show altitude separation and downrange separation versus time, respectively. In both altitude and downrange separation, debris trajectories achieve both positive and negative separation distances. In particular, the maximum-drag-minimum-lift case has both negative altitude and downrange separation at the same point in time, while the minimum-drag-maximum-lift case has both positive altitude and downrange separation at the same point in time. These results show that there exist possible debris trajectories with drag and lift-to-drag ratios between the simulated extremum trajectories that will recontact the descent vehicle during the gravity turn. Therefore, these results show that under the most conservative assumptions, direct far-field recontact risks exist for the hinged exit transition scheme.

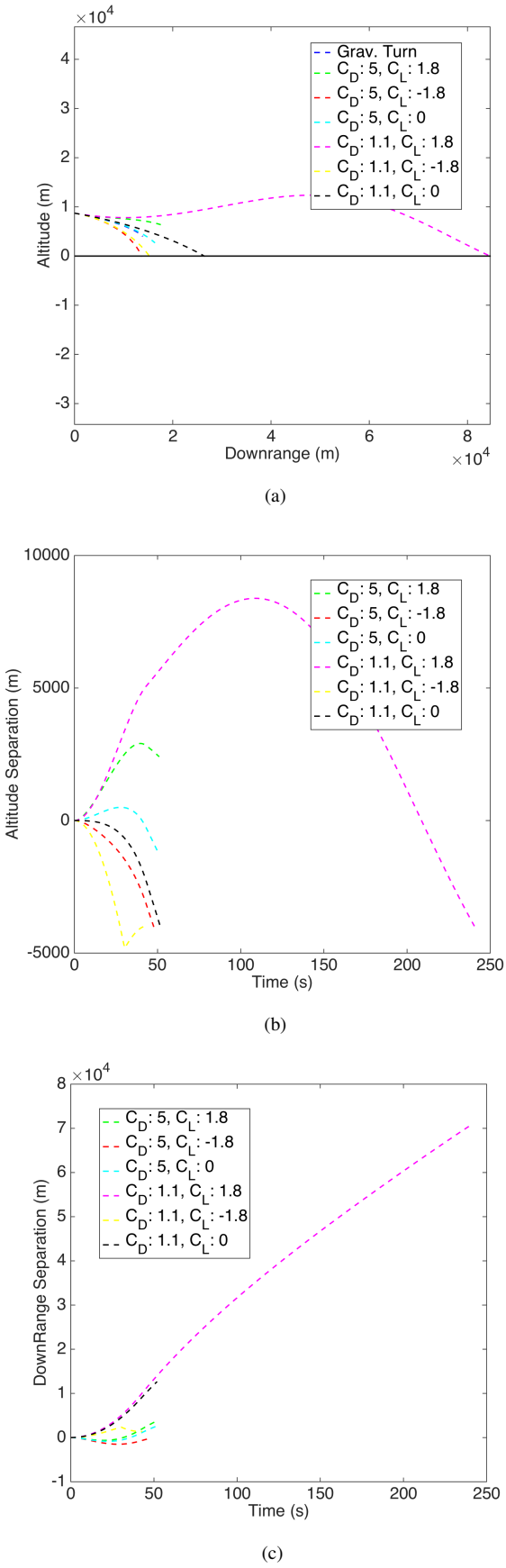

Figure 6. Trajectory dispersions for the aft-shell of the front exit transition scheme

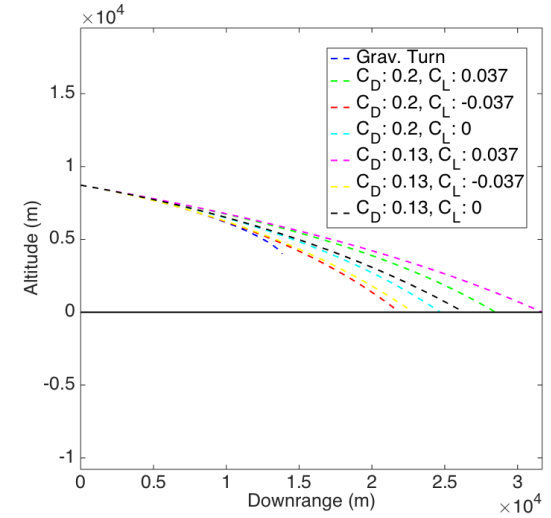

(a)

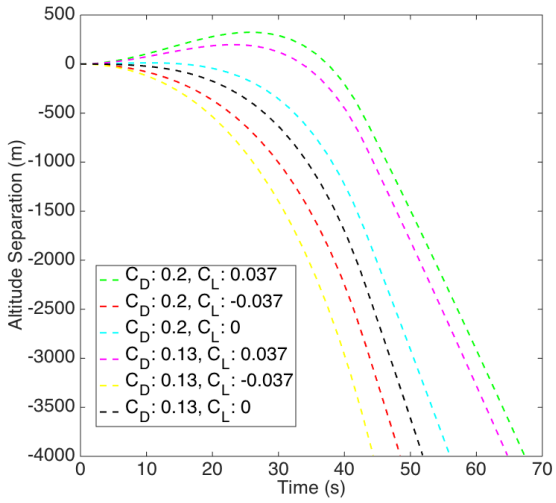

(b)

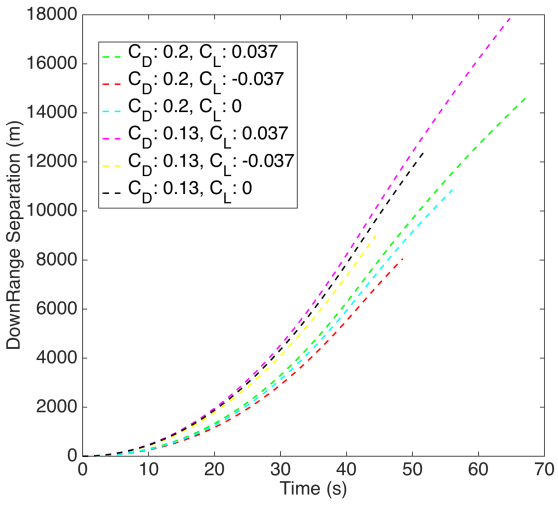

(c)

Figure 7. Trajectory dispersions for the hemispherical cap of the front exit transition scheme

Front Exit Maneuver

The front exit transition scheme is modeled and simulated using the same assumptions and methods as the hinged exit transition scheme. However, as opposed to the hinged exit scheme, the front exit scheme ejects two pieces of debris that are not identical to one another. Therefore, far-field recontact risks of each piece of debris must be individually investigated. Figures 6 and 7 show simulated results for the pieces of debris designated "aft shell" and "hemispherical cap", respectively.

The trajectories shown in figure 6 for the aft shell result in the same conclusions drawn from the hinged exit scheme debris trajectories. Figure 6(a) shows that in the absence of descent vehicle divert maneuvers or debris flight control schemes, the aft shell debris landing footprint poses a direct threat to the descent vehicle landing site and any pre-deployed landed assets near the descent vehicle landing site. Figures 6(b) and 6(c) show that under the most conservative assumptions, direct far-field recontact risks exist between the descent vehicle and the aft shell piece of debris for the front exit transition scheme.

Unlike the aft shell piece of debris, the hemispherical cap does not pose far-field recontact risks to the descent vehicle. Figure 7 shows that at all times after debris ejection, the hemispherical cap has positive downrange separation distance from the descent vehicle for all simulated extremum trajectories. However, because the aft shell does pose far-field recontact risks, this transition scheme as a whole is considered to pose far-field recontact risks.

4. Conclusions

For the reference vehicle considered in this study, it has been shown that pitch-around maneuvers require high thrust levels from the reaction control system in order to perform the transition in a short amount of time. This analysis shows that required thrust levels range between 160 kN and 430 kN for transitions having angular accelerations between 1 deg/s^2 and 5 deg/s^2. Additionally, it has been show that modeling a transition as a free-fall for 20 seconds results in an overly conservative prediction of transition performance for a pitch-around maneuver. For the transition schemes presented in this study that involve supersonic solid mass ejections, it has been shown that ejected debris poses a far-field recontact risk to the descent vehicle and additionally poses a risk to any pre-deployed landed assets near the descent vehicle landing cite. Future research into supersonic vehicle configuration transitions will include analysis of near-field recontact risks and development of far-field mitigation strategies such as descent vehicle divert maneuvers and debris flight control.

References

[1] S. Dutta and R. D. Braun, "Preliminary statistical trajectory and atmosphere reconstruction of MSL entry, descent, and landing," *23rd AAS/AIAA space flight mechanics . . .*, 2013.

[2] G. Mendeck and L. McGrew, "Post-flight EDL entry guidance performance of the 2011 Mars science laboratory mission," *AIAA/AAS Space Flight Mechanics Meeting*, 2013.

[3] D. W. Way, R. W. Powel, A. Chen, A. D. Steltzner, A. M. S. Martin, P. D. Burkhart, and G. F. Mendeck, "Mars Science Laboratory: Entry, Descent, and Landing

System Performance," *2007 IEEE Aerospace Conference*, pp. 1–19, 2007.

[4] A. Cianciolo, J. L. Davis, D. R. Komar, and M. M. Munk, "Entry, Descent and Landing Systems Analysis Study: Phase 1 Report," National Aeronautics and Space Administration, 2010.

[5] A. M. Korzun, "Aerodynamic and performance characterization of supersonic retropropulsion for application to planetary entry and descent," Thesis (Ph.D.)–Aerospace Engineering, Georgia Institute of Technology, 2012., Atlanta, Ga, 2012.

[6] P. Hoffman, T. Rivillini, E. Slimko, and N. Dahya, "Preliminary Design of the Cruise, Entry, Descent, and Landing Mechanical Subsystem for MSL," *IEEE Aerospace Conference*, pp. 1–18, 2007.

ACKNOWLEDGMENTS

Funding for this research was generously provide by a NASA Space Technology Research Fellowship.

BIOGRAPHY

David Blette *received his B.S. in aerospace engineering and mechanics from the University of Minnesota - Twin Cities in 2011. He is currently a graduate research assistant and NASA Space Technology Research Fellow at the Georgia Institute of Technology. His current research interests include supersonic retropropulsion technologies, entry vehicle supersonic configuration transition events, and multibody dynamics.*

Dr. Robert D. Braun *serves as the David and Andrew Lewis Professor of Space Technology at the Georgia Institute of Technology. He has been a member of the Georgia Tech faculty since 2003 and leads an active research and educational program focused on the design of advanced flight systems and technologies for planetary exploration. He has contributed to the formulation, development, and operation of multiple space flight missions. He previously served as a leader and senior manager for several engineering organizations at NASA. In 2010-2011, he served as the first NASA Chief Technologist in more than a decade. In this capacity, he was the senior Agency executive for technology and innovation policy and programs and was responsible for creating the NASA Space Technology programs. From 1989 to 2003, he was a member of the technical staff of the NASA Langley Research Center.*